

## Harder than Diamond: Superior Indentation Strength of Wurtzite BN and Lonsdaleite

Zicheng Pan,<sup>1</sup> Hong Sun,<sup>1,2,\*</sup> Yi Zhang,<sup>2</sup> and Changfeng Chen<sup>2,\*</sup>

<sup>1</sup>*Department of Physics, Shanghai Jiao Tong University, Shanghai 200030, China*

<sup>2</sup>*Department of Physics and High Pressure Science and Engineering Center, University of Nevada, Las Vegas, Nevada 89154, USA*

(Received 6 August 2008; published 6 February 2009)

Recent indentation experiments indicate that wurtzite BN (w-BN) exhibits surprisingly high hardness that rivals that of diamond. Here we unveil a novel two-stage shear deformation mechanism responsible for this unexpected result. We show by first-principles calculations that large normal compressive pressures under indenters can compel w-BN into a stronger structure through a volume-conserving bond-flipping structural phase transformation during indentation which produces significant enhancement in its strength, propelling it above diamond's. We further demonstrate that the same mechanism also works in lonsdaleite (hexagonal diamond) and produces superior indentation strength that is 58% higher than the corresponding value of diamond, setting a new record.

DOI: [10.1103/PhysRevLett.102.055503](https://doi.org/10.1103/PhysRevLett.102.055503)

PACS numbers: 81.40.Jj, 62.20.-x

Diamond is widely regarded as the hardest of all materials known. Over the past decades extensive theoretical [1–3] and experimental [4] efforts have been devoted to finding materials that are harder and thermally more stable than diamond. It was recently reported [5] that a nanocomposite containing a mixture of cubic and wurtzite (w-) BN reached the same level of indentation hardness as diamond. Cubic boron nitride (c-BN) is the second hardest material known, but its strength and hardness are well below those of diamond [4,6,7]. The experimental result thus suggests that w-BN may be as hard or harder than diamond, which came as a surprise since w-BN and c-BN have a similar bond length, elastic moduli, and ideal tensile and (pure) shear strength [8]. A nanoscale size effect was invoked [5] to explain the observed phenomenon. However, a similar ternary B-C-N nanocomposite exhibits hardness well below that of diamond [9], suggesting that the size effect may not be the only relevant mechanism at work here. To understand the unexpectedly high indentation hardness of w-BN, it is essential to examine its intrinsic structural and stress response to indentation loading. Here we show by first-principles calculations that large normal compressive pressures under indenters can compel w-BN into a stronger structure through a volume-conserving bond-flipping structural phase transformation during indentation. It significantly increases the indentation strength of w-BN to above the diamond value. This represents the first case where a material exceeds diamond in strength under the same loading condition. We further demonstrate that this novel mechanism also works in lonsdaleite (hexagonal diamond, that is isostructural to w-BN), producing a new record in indentation strength that is 58% higher than the corresponding value of diamond.

Recent developments have made it possible to calculate stress-strain relations and determine the peak strengths (ideal strengths) of perfect crystals under various loading conditions from first principles [6,7,10–19]. Such ideal strengths determined for perfect crystals set an upper limit

for material strengths, with ideal tensile strengths related to cleavage processes [11] and the ideal shear strengths to hardness tests. Experimentally, well-controlled nanoindentation results could approach calculated ideal shear strengths [20–22]. However, in most of the previous ideal shear strength calculations, pressures under indenters normal to indentation crystal planes are neglected, which gives rise to certain degrees of ambiguity when the calculated (pure) ideal shear strengths are compared to hardness results obtained using different types of indenters. To include the main effects of indenters' geometry in the calculations of ideal shear strengths, we introduce the ideal indentation strength for an indented material as the peak shear stress in the stress-strain relation on the easy cleavage plane in the weakest shear direction under biaxial stresses containing a shear and a normal compressive component. The ratio of the shear stress and the normal compressive pressure is determined by the relation  $\sigma_{zz} = \sigma_{xz} \tan\Psi$ , where  $\Psi$  is the centerline-to-face angle of the indenter [10]. The reason for defining ideal indentation strength on easy cleavage planes is that they form the most ubiquitous and stable exposed surfaces in bulk or nanoscale crystallites. Under indentation, shear instability usually precedes the initiation of cracks and dislocations [23], signaling the onset of incipient plasticity [14,16]; compressive pressure failure can also occur under biaxial stresses [10]. Our first-principles calculations show that w-BN and lonsdaleite exhibit higher ideal indentation strengths on their cleavage planes than diamond and unveil the underlying mechanism by identifying a novel two-stage biaxial shear deformation mode, where the materials become stronger during the first stage of structural phase transformations. These results account for the high indentation hardness of w-BN and predict lonsdaleite as the new hardest material as probed by ideal indentation strength.

In the present work, we calculate the ideal indentation strength of w-BN and lonsdaleite using the PARATEC codes [24] based on total-energy calculations with the local-

density-approximation (LDA) pseudopotential scheme, the plane-wave basis set [25–27] and the norm-conserving Troullier-Martins pseudopotentials [28]. The exchange-correlation functional of Ceperley and Alder [26] as parametrized by Perdew and Zunger [29] was used. The total energy of the structures was minimized by relaxing the structural parameters using a quasi-Newton method [30]. The unit cells of w-BN and lonsdaleite used in the calculations are illustrated in Fig. 1. The calculated stresses are accurate to within 0.1 GPa with a cutoff energy  $E_{\text{cut}} = 100$  Ry and a  $10 \times 10 \times 16$   $k$ -point grid based on the convergence tests. The quasistatic indentation strength and relaxed loading path were determined using a method described previously in which the biaxial stress under the indenter is projected into a shear stress (as  $x$  direction) and a compressive pressure (as  $z$  direction) component [10]. The lattice vectors were incrementally deformed in the direction of the applied shear strain. At each step, a small shear strain ( $\tau_{xz} = 0.005$ ) is applied in the chosen shear direction in the easy slip (or cleavage) plane and held fixed during the structural relaxation, which determines the calculated shear stress ( $\sigma_{xz}$ ), while the other five independent components of the strain tensor and all the atoms inside the unit cell were simultaneously relaxed until (i) the stress normal to the easy slip plane reached a specified value (i.e.,  $\sigma_{zz} = \sigma_{xz} \tan \Psi$ , where  $\Psi = 68^\circ$  is the centerline-to-face angle of the Vickers indenter), (ii) all the other four components of the Hellmann-Feynman stress tensor are less than 0.1 GPa, and (iii) the force on each atom becomes negligible. The shape of the (deformed) unit cell is determined completely at each step by this constrained atomic relaxation.

We first set out to determine the easy cleavage plane of w-BN and lonsdaleite by calculating their ideal tensile strength along several high-symmetry directions. The calculated results shown in Fig. 1 clearly indicate that the

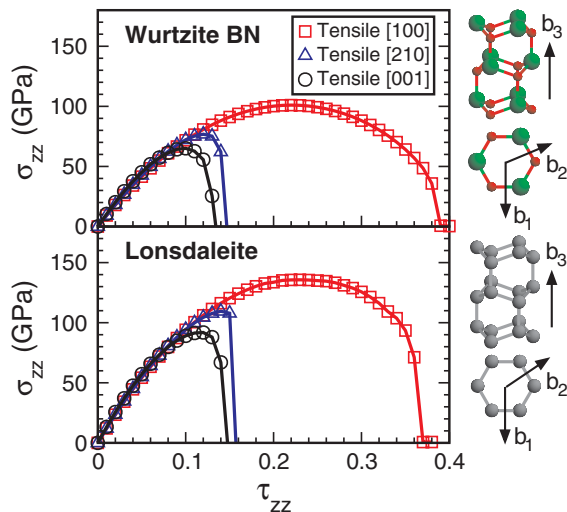


FIG. 1 (color online). Calculated tensile stress ( $\sigma_{zz}$ ) versus tensile strain ( $\tau_{zz}$ ) for wurtzite BN and lonsdaleite. The structural unit cells and axes are shown to the right of each panel.

weakest peak tensile stress occurs in the [001] direction in both cases, giving rise to the (001) easy cleavage planes. It is also noticed that the anisotropy in tensile strength of w-BN and lonsdaleite are much lower than their cubic counterparts, c-BN and diamond [7] caused by subtle differences in the directional arrangements of bonds in w-BN and lonsdaleite that significantly reduces the tensile strength anisotropy. More important, as we will show below, these subtle structural differences play a pivotal role in producing a novel two-stage shear deformation mode that is responsible for considerable strength enhancement under indentation.

We next examine the structural response under the biaxial indentation stresses to determine the ideal indentation strength of w-BN. For a better understanding of the deformation behavior, it is instructive to first examine the stress-strain relation and the ideal strength under pure shear deformation ( $\sigma_{zz} = 0$ ). The calculated results for w-BN are shown in Fig. 2(a) together with the results for c-BN. For c-BN there are two inequivalent shear directions in its easy cleavage (111) plane, resulting in an easy and a hard shear direction [7] with the former setting the (pure) ideal shear strength. For w-BN, the weakest pure shear direction is [210] on the (001) plane [8] which has a sixfold rotation symmetry. The (pure) ideal shear strength of w-BN is very close to that of c-BN. Despite differences in bonding structure, w-BN also undergoes a graphitization process [indicated by points  $P_2$  and  $P_3$  in Fig. 2(b)] similar to c-BN beyond its elastic limit with a large volume expansion [see lower panel of Fig. 2(a)] that is characteristic of such a process [7]. However, it is noticed that the bond and volume expansion of w-BN under pure shear deformation occurs in the direction normal to the easy cleavage plane. Under indentation the large compressive pressure that is aligned in the same direction severely impedes and prevents such bond and volume expansion. As a result, new deformation modes with distinct structural properties may appear. This is indeed what happens in w-BN as revealed by our calculations. Results presented in Fig. 2(c) and 2(d) reveal a novel two-stage shear deformation process. The first is similar to the pure shear mode except for an overall compression of the structure in the direction of indentation. At the shear strain of 31% where graphitization occurs under pure shear mode [point  $B_2$  in Fig. 2(c) which coincides with point  $P_2$  in Fig. 2(a)], a bond-flipping transformation to a structure with lower energy [see Fig. 2(d)] occurs. It completely releases the shear stress built up during the first stage of shear deformation. There is no volume change associated with this transformation [same volume at points  $B_2$  and  $B_3$  shown in Fig. 2(c)], indicating short valence bonds as before. As a result, the structure remains strong (in fact, it becomes stronger). Further indentation leads to the second stage of shear deformation. A salient point here is that after the bond-flipping transformation the structure of w-BN closely resembles that of c-BN and, most importantly, the second stage shear mode is along the hard shear direction of the c-BN structure. This

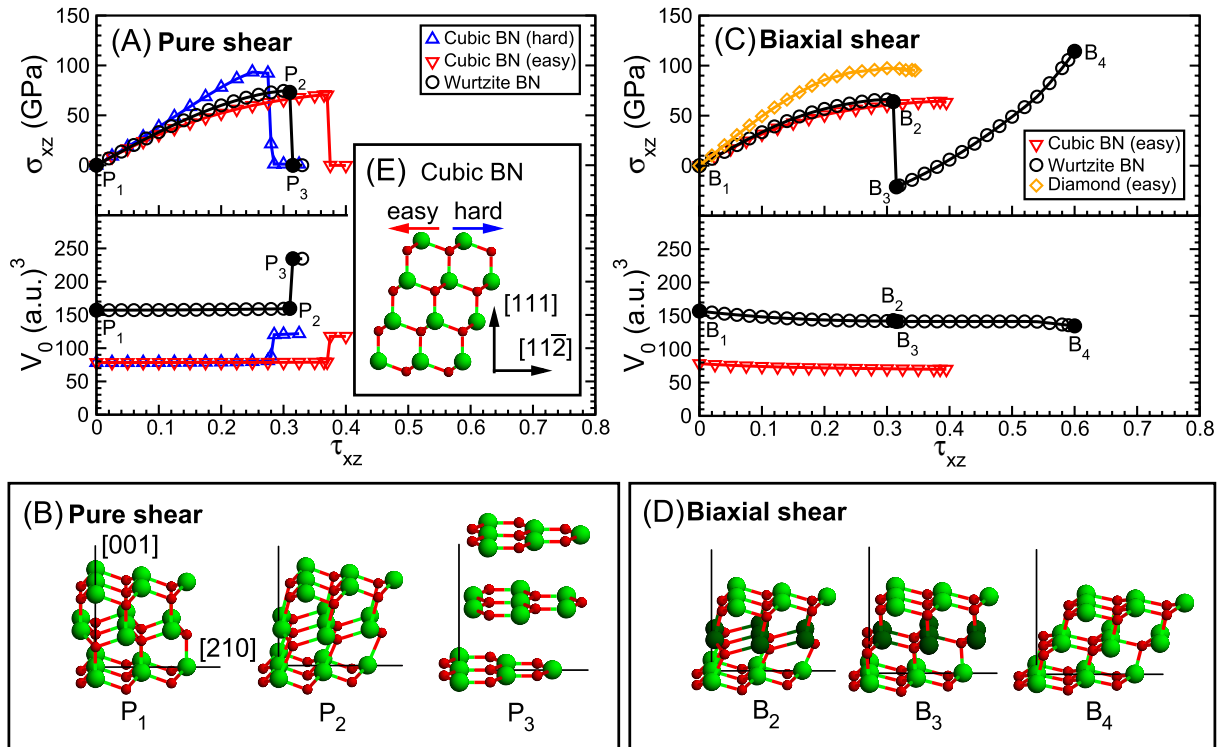


FIG. 2 (color online). Calculated shear stress ( $\sigma_{xz}$ ) and unit cell volume ( $V_0$ ) versus shear strain ( $\tau_{xz}$ ) for w-BN compared to those of c-BN under pure shear (A) and biaxial shear (C) modes. Corresponding snapshots of selected bonding configurations at key deformation points are presented in (B) and (D), respectively. The easy and hard shear directions of c-BN are indicated in (E). For comparison, the stress-strain curve for diamond along the easy shear direction under the biaxial stress is also shown in (C).

can be seen by comparing the structural snapshots shown in Fig. 2(d) for w-BN after the transformation and in Fig. 2(e) for c-BN. Since the (001) plane of w-BN has a sixfold rotation symmetry, the second stage hard shear resistance occurs in all six equivalent (001) $\langle$ 210 $\rangle$  directions when the indenter pushes outwards on the indented (001) plane. This process leads to significantly enhanced indentation strain and strength that reach 114 GPa at the peak (point  $B_4$ ) which is a 78% increase from the peak value before the bond-flipping occurs (right before point  $B_2$ ). Most significantly, this pushes it well above the value (97 GPa) for diamond under the same indentation condition. This result may explain the recent experimental indentation results that indicate w-BN is comparable to or harder than diamond under indentation [5]. Structural phase transformations into superhard structures under moderate normal pressures have been reported previously in experiments. For instance, graphite with similar hexagonal symmetry like w-BN (or lonsdaleite) can transform into a superhard structure (different from that of lonsdaleite and diamond) harder than diamond under uniaxial normal pressure along its  $c$  axis at ambient temperature when the applied pressure reaches above 17 GPa [31], which is much lower comparing to the compressive pressures under indenters in the indentation processes on w-BN (or lonsdaleite).

We now turn to lonsdaleite that is isostructural to w-BN and, therefore, may exhibit superior indentation strength

compared to diamond if the same mechanism works here. Our calculations (see Fig. 3) demonstrate that the same bond-flipping transformation occurs after the tendency for graphitization is impeded by the normal compressive pressure. A two-stage shear deformation mode ensues, yielding an indentation strength of 152 GPa, which is 58% higher than the corresponding value (97 GPa) of diamond. This remarkable result produces a new record for indentation strength on the easy cleavage plane among all known materials, followed (at a distance) by w-BN. It is noted that lonsdaleite exhibits almost identical ideal tensile strength and only slightly larger pure ideal shear strength compared to diamond. The significant enhancement in its indentation strength occurs under biaxial stress loading conditions. The situation in w-BN versus c-BN is similar. All past calculations have shown that diamond exhibits the highest strength under various loading conditions compared to other materials, which was consistent with all available measurements. Here we show for the first time that w-BN and lonsdaleite exhibit higher strength than diamond under indentation.

For a complete study of w-BN and lonsdaleite, synthesis of large-size samples remains a major challenge. Both have been synthesized before, mostly in small quantities [32–34]. The recent report on the nanocomposite of c-BN and w-BN mixture [5] represents a promising direction. This approach may also prove effective for producing nano-

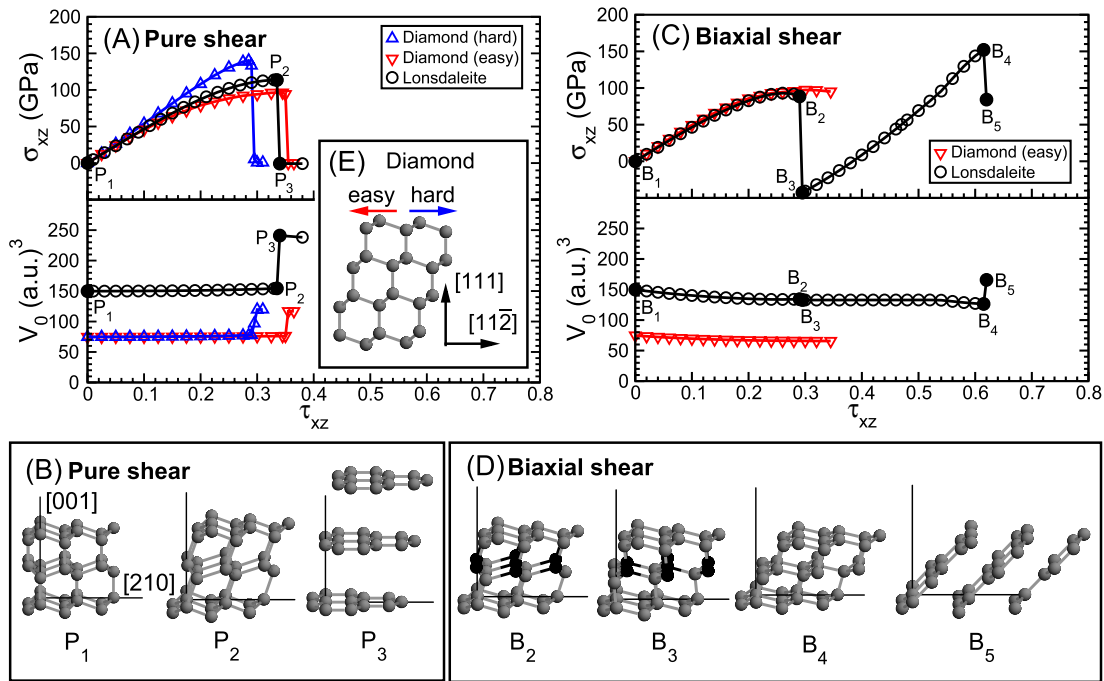


FIG. 3 (color online). Calculated stress ( $\sigma_{xz}$ ) and unit cell volume ( $V_0$ ) versus strain ( $\tau_{xz}$ ) for lonsdaleite compared to those of diamond under pure shear (A) and biaxial shear (C) modes. Corresponding snapshots of selected bonding configurations at key deformation points are presented in (B) and (D), respectively. The easy and hard shear directions of diamond are indicated in (E).

composites containing lonsdaleite and diamond mixture. Another promising approach is to grow samples on appropriately chosen substrates, as recently demonstrated for lonsdaleite on h-GaN [35]. While improvements in material synthesis still needs further work, the results reported here reveal the nature of intriguing atomistic mechanism for the observed indentation hardness of w-BN and predicted new hardest indentation strength level of lonsdaleite, where structural phase transformations into stronger structures in indentation can enhance greatly the strengths of certain materials. It offers insights for a new approach in designing superhard materials.

Work supported by DOE Grant No. DE-FC52-06NA26274 and National Natural Science Foundation of China Grant No. 10874112.

\*Corresponding authors.

hsun@sjtu.edu.cn

chen@physics.unlv.edu

- [1] A. Y. Liu and M. L. Cohen, *Science* **245**, 841 (1989).
- [2] D. M. Teter and R. J. Hemley, *Science* **271**, 53 (1996).
- [3] R. B. Kaner *et al.*, *Science* **308**, 1268 (2005).
- [4] V. V. Brazhkin *et al.*, *Philos. Mag. A* **82**, 231 (2002).
- [5] N. Dubrovinskaia *et al.*, *Appl. Phys. Lett.* **90**, 101912 (2007).
- [6] Y. Zhang *et al.*, *Phys. Rev. Lett.* **94**, 145505 (2005).
- [7] Y. Zhang *et al.*, *Phys. Rev. B* **73**, 144115 (2006).

- [8] R. F. Zhang *et al.*, *Phys. Rev. B* **77**, 172103 (2008).
- [9] Y. S. Zhao *et al.*, *J. Mater. Res.* **17**, 3139 (2002).
- [10] Z. C. Pan *et al.*, *Phys. Rev. Lett.* **98**, 135505 (2007).
- [11] R. H. Telling *et al.*, *Phys. Rev. Lett.* **84**, 5160 (2000).
- [12] H. Chacham *et al.*, *Phys. Rev. Lett.* **85**, 4904 (2000).
- [13] S. H. Jhi *et al.*, *Phys. Rev. Lett.* **87**, 075503 (2001).
- [14] S. Ogata *et al.*, *Science* **298**, 807 (2002).
- [15] D. M. Clatterbuck *et al.*, *Phys. Rev. Lett.* **91**, 135501 (2003).
- [16] S. Ogata *et al.*, *Phys. Rev. B* **70**, 104104 (2004).
- [17] X. Blase *et al.*, *Phys. Rev. Lett.* **92**, 215505 (2004).
- [18] M. G. Fyta *et al.*, *Phys. Rev. Lett.* **92**, 215505 (2004).
- [19] Y. Zhang *et al.*, *Phys. Rev. Lett.* **93**, 195504 (2004).
- [20] C. R. Krenn *et al.*, *Phys. Rev. B* **65**, 134111 (2002).
- [21] M. I. Eremets *et al.*, *Appl. Phys. Lett.* **87**, 141902 (2005).
- [22] T. Li *et al.*, *Phys. Rev. Lett.* **98**, 105503 (2007).
- [23] A. Gouldstone *et al.*, *Acta Mater.* **48**, 2277 (2000).
- [24] <http://www.nersc.gov/projects/paratec/>
- [25] J. Ihm *et al.*, *J. Phys. C* **12**, 4409 (1979).
- [26] D. M. Ceperley *et al.*, *Phys. Rev. Lett.* **45**, 566 (1980).
- [27] M. L. Cohen, *Phys. Scr.* **T1**, 5 (1982).
- [28] N. Troullier and J. L. Martins, *Phys. Rev. B* **43**, 1993 (1991).
- [29] J. P. Perdew *et al.*, *Phys. Rev. B* **23**, 5048 (1981).
- [30] B. G. Pfrommer *et al.*, *J. Comput. Phys.* **131**, 233 (1997).
- [31] W. L. Mao *et al.*, *Science* **302**, 425 (2003).
- [32] F. P. Bundy *et al.*, *J. Chem. Phys.* **38**, 1144 (1963).
- [33] C. S. Yoo *et al.*, *Phys. Rev. B* **56**, 140 (1997).
- [34] H. He *et al.*, *Appl. Phys. Lett.* **81**, 610 (2002).
- [35] A. Misra *et al.*, *Appl. Phys. Lett.* **89**, 071911 (2006).